Synthesis and Optical and Transport Properties of a Phenyl-Substituted Polythiophene

SIRAYE E. DEBEBE,[1] DESTA A. GEDEFAW,[1] WENDIMAGEGN MAMMO,[1] TEKETEL YOHANNES,[1] FRANCESCA TINTI,[2] ALBERTO ZANELLI,[2] VALERIA FATTORI,[2] NADIA CAMAIONI[2]

[1]Department of Chemistry, Addis Ababa University, P.O. Box 1176, Addis Ababa, Ethiopia

[2]Istituto per la Sintesi Organica e la Fotoreattività, Consiglio Nazionale delle Ricerche, via P. Gobetti 101, I-40129 Bologna, Italy

Received 22 February 2011; accepted 1 April 2011
DOI: 10.1002/pola.24701

ABSTRACT: The synthesis and characterization of a novel polythiophene substituted with a 2′-pentyloxy-5′-(1‴-oxooctyl) phenyl group (PPOPT) is reported. The bulk transport properties of thin films of PPOPT are investigated by admittance spectroscopy. The dramatic effect of the phenyl side chain on the mobility of positive carriers in films of PPOPT is described. The photophysics of PPOPT in both solution and thin film is also investigated and correlated to substituent-driven intrachain and interchain arrangements. © 2011 Wiley Periodicals, Inc. J Polym Sci Part A: Polym Chem 49: 2693–2699, 2011

KEYWORDS: admittance spectroscopy; charge transport; conjugated polymers; phenyl substitution; photophysics; polythiophene

---

INTRODUCTION An intensive research activity on π-conjugated polymers has been stimulated by the prospect of low-cost fabrication of plastic electronic devices, since their discovery in 1977. A notable feature of conjugated polymers lies in the versatility of their molecular structure which affords wide space to prepare new materials with improved properties.[1] Polythiophene and its derivatives constitute one of the most promising class of conjugated polymers and have been widely used in solution-processed polymer solar cells[2] and field-effect transistors,[3] as well as in the fabrication of light-emitting diodes.[4]

To tune their electronic properties to meet the request for different applications, chemical modifications of polythiopene derivatives are performed. One method to tailor the electronic properties is the introduction of substituents on the thiophene rings.[5] Substituents can influence the electrical, electrochemical, and optical properties of the resulting polymers, other than modifying their processability in organic solvents. Depending on their nature, size and position, substituents can affect the interaction between polymer chains or induce a distortion of the polymer backbone, resulting in the variation of the π conjugation of the aromatic system.

Phenyl-substituted polythiophenes have already been reported in the literature, showing how the phenyl substituents affect the electrochemistry,[6] the light emission properties,[7] as well as the photoinduced charge transfer behavior.[8] However, the effect of the phenyl substitution on the transport properties of this class of polythiophenes has not been thoroughly investigated. In this article, we report the synthesis and characterization of a novel phenyl-substituted polythiophene, poly[3-(2′-pentyloxy-5′-(1‴-oxooctyl) phenyl) thiophene] (PPOPT). In addition to the optical and electrochemical characterization, the investigation of bulk transport properties of positive carriers in thin films of PPOPT is described.

EXPERIMENTAL

Synthesis of the Polymer

Synthesis of 1-Bromo-2-pentyloxybenzene (2)

To a mixture of *o*-bromophenol (5 g, 0.03 moles) in 30 mL dimethylformamide, anhydrous potassium carbonate (4.14 g, 0.03 moles) was added. The mixture was stirred, and 1-bromopentane (4.53 g, 0.03 moles) was added gradually with heating over an oil bath. The mixture was heated overnight, cooled to room temperature, and filtered by suction. The filtrate was acidified with 2 M HCl and extracted with diethyl ether. The ether extract was washed with 1 M NaOH and water and was dried over anhydrous Na_2SO_4. The ether was removed by rotary evaporator to afford 1-bromo-2-pentyloxybenzene (**2**) as a yellowish oil (6 g, 82.3%).

^1H NMR ($CDCl_3$, 400 MHz): δ 7.45 (*dd*, $J = 8$, 1.36 Hz, 1H), 7.15 (m, 1H), 6.8 (*dd*, $J = 8$, 1.36 Hz, 1H), 6.7 (m, 1H), 3.9 (*t*, 2H), 1.75 (*m*, 2H), 1.45 (*m*, 2H), 1.35 (*m*, 2H), 0.85 (*t*, 3H). ^{13}C NMR ($CDCl_3$, 100 MHz): δ 156.0, 133.7, 128.8, 122.0, 113.7, 112.7, 69.6, 29.3, 28.6, 22.9, 14.5.

Correspondence to: W. Mammo (E-mail: wmammo@chem.aau.edu.et) or N. Camaioni (E-mail: camaioni@isof.cnr.it)
Journal of Polymer Science Part A: Polymer Chemistry, Vol. 49, 2693–2699 (2011) © 2011 Wiley Periodicals, Inc.

Synthesis of 1-Bromo-2-pentyloxy–5-(1″-oxooctyl) benzene (3)

In a two-necked round-bottomed flask, 1-bromo-2-pentyloxybenzene (**2**) (6 g, 0.025 moles), aluminum chloride (3.34 g), and carbon disulfide (25 mL) were mixed. A condenser was attached to one of the necks of the flask and to the other, a dropping funnel containing octanoyl chloride (4.1 g, 0.025 moles) was added. Both the condenser and the dropping funnel were protected with calcium chloride guard tubes. The octanoyl chloride was added drop by drop for 30 min with continuous stirring of the contents of the flask. The mixture was refluxed for 6 h until the evolution of hydrogen chloride gas almost ceased. The solvent was removed by distillation, and the remaining mixture was poured into a beaker containing 13 g of crushed ice and concentrated HCl (8 mL). The mixture was stirred and extracted with diethyl ether. The ether extract was washed with water (twice), 10% NaOH solution (once) and water (twice) and dried over anhydrous sodium sulfate. The ether was removed by rotary evaporator to yield **3** as an orange colored solid (6 g, 65%).

mp 33.3–35.4 °C. ^{1}H NMR (CDCl$_3$, 400 MHz): δ 8 (*d*, J = 1.26 Hz, 1H), 7.81 (*dd*, J = 8.86, 1.26 Hz, 1H), 6.84 (*d*, J = 8.86 Hz, 1H), 4.1 (*t*, 2H), 2.85 (*t*, 2H), 1.8–1.0 (*m*, 16H), 1.1–0.8 (*m*, 3H), 0.8 (*t*, 3H). ^{13}C NMR (CDCl$_3$, 100 MHz): δ 198.0, 159.4, 133.8, 131.2, 129.4, 112.6, 112.2, 69.7, 38.5, 32.1, 29.7, 29.5, 29.0, 28.5, 24.8, 23.0, 22.7, 14.4, 14.3. Infrared (IR) $\nu_{\max}$ (cm^{-1}): 2950, 2875, 1700, 1600, 1500, 1290, 1080, 800–500.

Synthesis of 3-[2′-Pentyloxy-5′-(1‴-oxooctyl)phenyl] thiophene (4)

In a one-necked round-bottomed flask kept under nitrogen atmosphere, Pd(PPh$_3$)$_4$ (0.25 g), 1-bromo-2-pentyloxy–5-(1″-oxooctyl)benzene (**3**) (4.03 g, 0.01 mol), and 1,2-dimethoxy ethane (50 mL) were added, and the mixture was stirred for 10 min. 3-Thiopheneboronic acid (1.40 g, 0.01 mol) was then added followed by the addition of 1 M sodium bicarbonate (40 mL). The mixture was refluxed monitoring the progress of the reaction by thin layer chromatography. After 5 h, the reaction mixture was cooled, and the 1,2-dimethoxy ethane was removed by rotary evaporator. Water (100 mL) was added to the residue, and the mixture was extracted with diethyl ether five times. The ether extract was washed with distilled water, dried over anhydrous Na$_2$SO$_4$, and the ether was removed to afford dark-brown oil (5.57 g), which solidified on standing. The crude product was chromatographed over a short column of silica gel using petroleum ether as eluent. Compound **4** (2.10 g, 51.7%) was obtained in pure form as white needle-like crystal after recrystallization from acetone–methanol.

mp 61.3–63.1°C. ^{1}H NMR (CDCl$_3$, 400 MHz): δ 8.05 (*d*, J = 1.95 Hz, 1H), 7.88 (*dd*, J = 7.8, 1.95 Hz, 1H), 7.58 (*dd*, J = 3.20, 1.0 Hz, 1H), 7.4 (*dd*, J = 5.6, 1.0 Hz, 1H), 7.25 (*dd*, J = 7.80, 2.34 Hz, 1H), 6.88 (*d*, J = 7.80 Hz, 1H), 4.0 (*t*, 2H), 2.85 (*t*, 2H), 1.9–1.0 (*m*, 16H), 0.9 (*m*, 6H). ^{13}C NMR (CDCl$_3$, 100 MHz): 199.6, 160.1, 137.9, 130.4, 130.3, 129.4, 128.8, 125.4, 124.9, 124.1, 111.9, 69.2, 38.7, 32.1, 29.8, 29.6, 29.2, 28.6, 25.1, 23.0, 22.8, 14.5, 14.4. IR $\nu_{\max}$ (cm^{-1}): 2950, 2875, 1700, 1600, 1500, 1290, 1080, 800–500.

Synthesis of Poly[3-(2′-pentyloxy-5′-(1‴-oxooctyl) phenyl)thiophene] (5)

Compound **4** (0.5 g, 1.45 mmol) was dissolved in chloroform (15 mL) and a slurry of ferric chloride (1.32 g) in chloroform (15 mL) was added to it for 90 min, and the mixture was stirred for an extra 3.5 h. The reaction mixture was poured into methanol, and the red precipitate was collected by suction filtration. The solid material was dissolved in chloroform and was washed with concentrated aqueous ammonia solution (six times), with 0.05 M EDTA (twice) and finally with distilled water (twice) and filtered using a sintered glass funnel. The chloroform solution was concentrated to a small volume and poured into methanol and the polymer that precipitated was collected by suction filtration. Polymer **5** was obtained as red powder (270 mg).

mp > 250 °C. $M_{\rm n}$ = 50,500, $M_{\rm w}$ = 92,000. ^{1}H NMR (CDCl$_3$, 400 MHz) (partial data): δ 7.9 (*d*, 1H), 7.7 (*d*, 1H), 6.8 (*d*, 1H), 6.5 (*s*, 1H), 3.8 (*t*, 2H), 2.75 (*t*, 2H), 0.5–2.0 (*unresolved*, aliphatic protons); IR $\nu_{\max}$ (cm^{-1}): 2950, 2875, 1700, 1600, 1500, 1290, 1100, 900–675.

Optical and Electrochemical Characterization

UV–Vis absorption spectra were recorded with a Perkin Elmer 950 spectrophotometer. Photoluminescence (PL) spectra, in solution and in thin film on quartz substrate, were obtained by using a Spex Fluorolog II 1681 spectrofluorometer. Quantum yields of PL for solutions were obtained as relative values using Ru(bipy)$_3$Cl$_2$ in aerated water solution as the reference, and an Edinburgh fluorometer equipped with a Labsphere integrating sphere was used to measure absolute quantum yields of PL of solid films.[9]

Cyclic voltammetries of thin films of PPOPT, spin coated onto indium tin oxide (ITO)-coated glass substrate (15 × 15 mm^2) from a chloroform solution, were recorded by an AMEL electrochemical system model 5000. A three-electrode system was used, consisting of a platinum wire as auxiliary electrode, aqueous saturated calomel (SCE), whose potential resulted −0.392 V versus ferrocene/ferricenium, as internal reference electrode,[10] and ITO as working electrode. The three electrodes were placed in an electrochemical cell consisting of three compartments separated by glass frits. A 0.1 mol L^{-1} tetrabutylammonium perchlorate (C$_4$H$_9$)$_4$NClO$_4$ (Fluka puriss., crystallized from CH$_3$OH and vacuum dried) in acetonitrile, CH$_3$CN (Merck Uvasol, stored under argon pressure and over molecular sieves 3 Å activated at 400 °C for 4 h) was used as supporting electrolyte. Argon gas was bubbled for 20 min in the working compartment before the measurement. During the measurement, argon gas was flushed into the working electrode compartment.

Characterization of Transport Properties

The devices used for admittance spectroscopy measurements were prepared in the sandwiched structure ITO/PEDOT:PSS/PPOPT/Al, where PEDOT:PSS is poly(3,4-ethylenedioxythiophene)/polystyrene sulfonic acid (CLEVIOS P VP AI 4083,

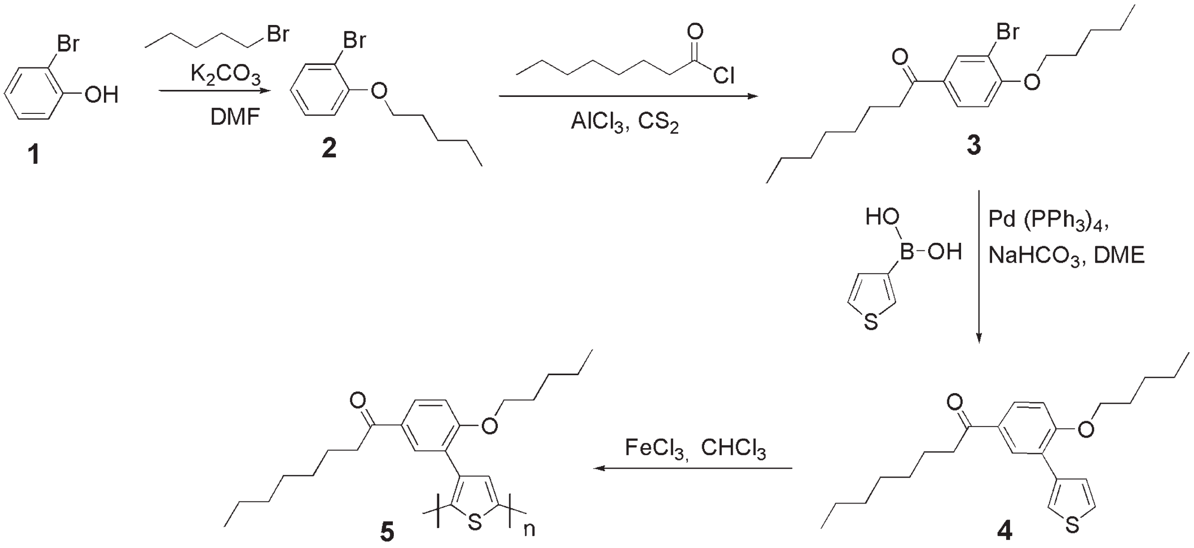

SCHEME 1 Scheme of the synthesis of poly[3-(2′-pentyloxy-5′-(1‴-oxooctyl) phenyl)thiophene] (PPOPT).

H.C. Starck). ITO/glass substrates were first cleaned in detergent and water, then ultrasonicated in acetone and isopropyl alcohol for 15 min each. The layer of PEDOT:PSS (around 40 nm) was spin coated at 4000 rpm onto ITO/glass substrates, then baked in an oven at 120 °C for 10 min. The polymer layer was spin coated at 850 rpm from a chloroform solution (22 g L^{-1}) and thermally annealed at 120 °C for 25 min in argon atmosphere before the deposition of top electrode. The thickness of the polymer layer, measured with a Tencor AlphaStep profilometer, was 260 nm. The top Al electrode (70 nm) was thermally evaporated at a base pressure of 4×10^{-6} mbar through a shadow mask giving an active device area of 0.25 cm^2.

The electrical characterization of the devices was carried out at room temperature under dynamic vacuum (5×10^{-5} mbar). Admittance was measured by using a Solartron 1255 Frequency Response Analyzer with a Solartron 1294 dielectric interface. The amplitude of the ac modulation voltage was 50 mV; the forward dc bias was varied in the range of 0–10 V with a voltage step of 1 V, and a frequency sweep range of $1–5 \times 10^5$ Hz was used.

RESULTS AND DISCUSSION

Scheme 1 shows the synthetic route to PPOPT (**5**). Thus, 2-bromophenol (**1**) was O-alkylated with 1-bromopentane to afford **2** in high yield. The Friedel–Crafts acylation of **2** with octanoyl chloride went smoothly in CS_2 to provide **3**. Compound **3** was then subjected to a Suzuki coupling reaction with freshly prepared 3-thiopheneboronic acid in the presence of $Pd(PPh_3)_4$ to give monomer **4**, which was subsequently polymerized using $FeCl_3$ in chloroform to afford **5** as a red powder. PPOPT is more soluble in organic solvents such as chloroform, chlorobenzene, and dichlorobenzene, leading to good film-forming properties when spin coated from the related solutions.

The ^1H NMR spectrum of PPOPT (not shown here) revealed a singlet peak in the aromatic region at δ 6.5, which is attributable to the thiophene ring proton. It can, therefore, be suggested that the polymer is regioregular,[11] and the coupling between the thiophene repeating units is mainly in a head-to-tail fashion. However, the substitution at C-3 of the polythiophene backbone could cause twisting of the phenyl rings out of plane, which could affect the packing of the polymer chain in the solid state.[12]

The optical properties of PPOPT were investigated by UV–Vis absorption and PL spectroscopy. The normalized spectra, in a diluted chloroform solution (10^{-5} mol L^{-1}) and in thin film spin coated onto quartz substrate, are shown in Figure 1. The polymer exhibits absorption maxima at 487 nm and at 501 nm, in solution and in thin film, respectively, leading to a red shift of 14 nm in the solid state. An optical energy gap of 2.0 eV was estimated from the absorption onset of the film. In addition, while the absorption spectrum in solution is structureless, the appearance of a relatively weak shoulder at ~580 nm is visible in the solid state. This feature, along with the moderate red shift of the spectrum when going from solution to thin film, is an indication of moderate interactions between the polymer chains in the solid state[13] or a larger overlap of π orbitals on the polymer backbone due to an increased coplanarity of the thiophene rings in the solid state induced by alignment of the alkyl chains.[14] The narrowing of the PL band in the solid state (full width at half-maximum is 0.25 eV in film and 0.36 eV in solution) seems to support a well-ordered solid state induced by the substituents on the phenyl ring.[15]

Stokes shifts are low and similar in solution and in film (0.38 eV in solution and 0.35 eV in film), suggesting a moderate distortion of the excited state with respect to the ground state.[16] Quantum yield of PL in solution (0.11) is relatively high pointing out a good planarity of the polymer backbone, accordingly, quantum yield of PL in solid state is

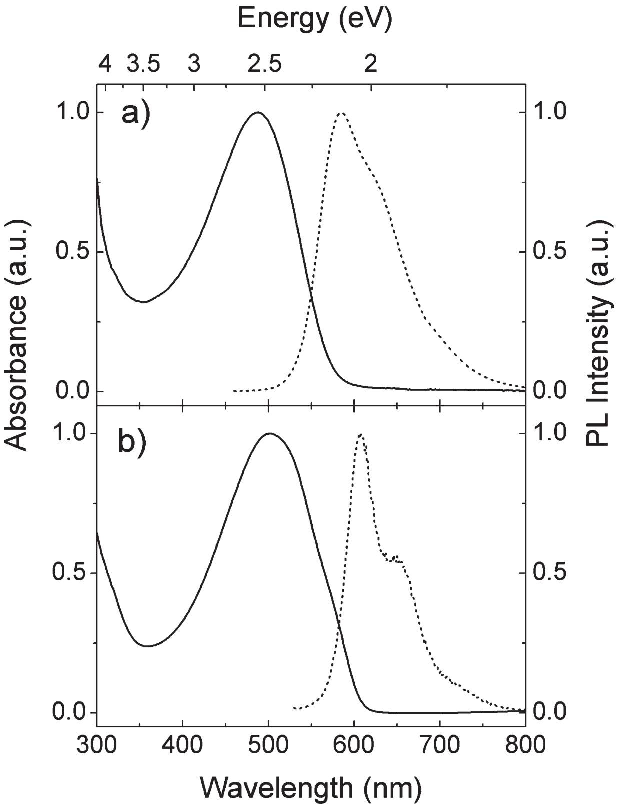

FIGURE 1 Normalized UV–Vis absorption and PL spectra of PPOPT in chloroform solution (a) and in spin-coated film onto quartz substrate (b). The excitation wavelengths were 445 and 500 nm, in solution and in film, respectively.

high (0.11) and this must be due to a well-ordered polymer backbone that is separated from neighboring chains, making the interchain interactions small. This is achieved with attachment of two side groups on the opposite ortho and meta positions of the phenyl ring which will force the phenyl out of the backbone plane, and thereby separate the polymer chains from each other.[15,17]

Electrochemical cyclic voltammetry measurements were carried out on PPOPT films spin coated onto ITO/glass substrate, used as working electrode. As shown in Figure 2, a quasi-reversible oxidation wave, with the onset potential of 0.81 V versus SCE, and a quasi-reversible reduction wave, with the onset potential of −1.54 V versus SCE, were observed. If compared to a similar phenyl-substitued polythiophene, poly(3-[2′-pentyloxy-5′-(octyl)phenyl]thiophene),[6] the relevant shift of the reduction wave toward less negative potentials (of around 0.5 V) could be attributed to the conjugation of ketone in meta position of the phenyl side group.

The energy levels of the highest occupied molecular orbital (HOMO) and the lowest unoccupied molecular orbital were calculated to be −5.49 and −3.14 eV, respectively, from the onset oxidation and reduction potentials, assuming the SCE level at −4.68 eV.[18] As often observed for conjugated polymers, the electrochemical energy gap was found to be slightly higher than the optical energy gap. This could be related to structural differences in the thin film due to swelling by the solvent or the exciton binding energy for conjugated polymers.[19]

Admittance spectroscopy[20] was used to investigate the bulk average hole mobility in thin film of PPOPT. In an admittance experiment, the charge relaxation driven by a small harmonic voltage modulation is probed and by superimposing a forward dc bias V_{dc} to the harmonic voltage, free carriers can be injected into a sample having a diode structure. Devices with the sandwich structure ITO/PEDOT:PSS/PPOPT/Al were prepared for this purpose. Under forward bias conditions (ITO positively biased), ITO/PEDOT:PSS electrode is able to inject holes into the HOMO level of the polymer, while an energy barrier for electron injection of around 1 eV is expected at the Al/PPOPT interface (Fig. 3). So, the aluminum top contact acts as an electron-blocking contact in the investigated hole-only devices under forward bias.

On injecting charge carriers, by applying a dc bias V_{dc} to the sample, dramatic changes are observed for admittance Y, given by:

$$Y(\omega) = G(\omega) + i\omega C(\omega) \qquad (1)$$

where G is the conductance, C the capacitance, i is the imaginary unit, and $\omega = 2\pi f$ is the angular frequency of the harmonic voltage.

As expected, conductance increases by increasing V_{dc}, as shown in Figure 4(a) for the sample ITO/PEDOT:PSS/PPOPT/Al; however, charge injection also affects capacitance spectra. Although, at zero bias (no injection) capacitance is nearly frequency independent, under high-injection conditions and for one-carrier devices, C usually shows a light minimum in the intermediate frequency range. As an example, the capacitance spectrum obtained for an ITO/PEDOT:PSS/PPOPT/Al sample at $V_{dc} = 5$ V is shown in Figure 4(b) and compared with that at $V_{dc} = 0$. The positive contribution to C in the low

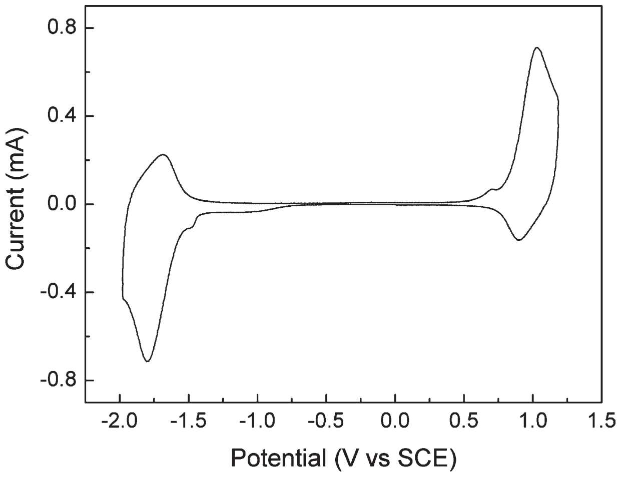

FIGURE 2 Cyclic voltammogram (fourth scan) of a PPOPT film, spin coated onto ITO/glass electrode, in $(C_4H_9)NClO_4$/acetonitrile supporting electrolyte at a scan rate of 100 mV s^{-1}.

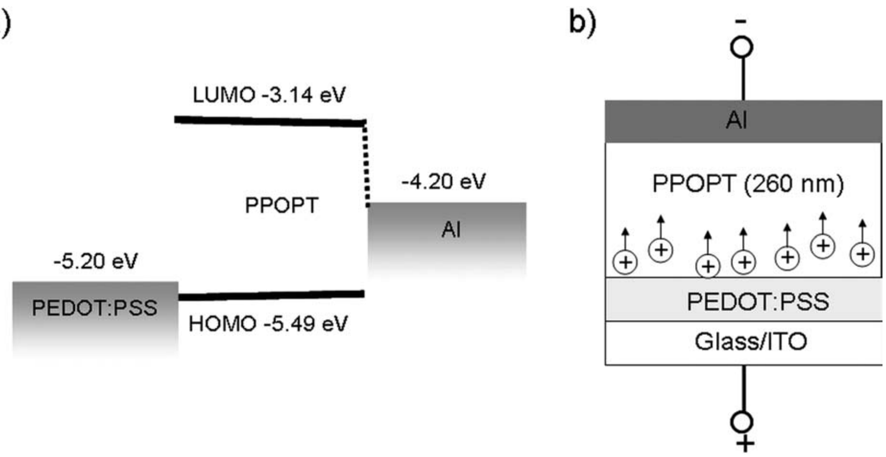

FIGURE 3 Energy diagram and structure of hole-only devices used in this study.

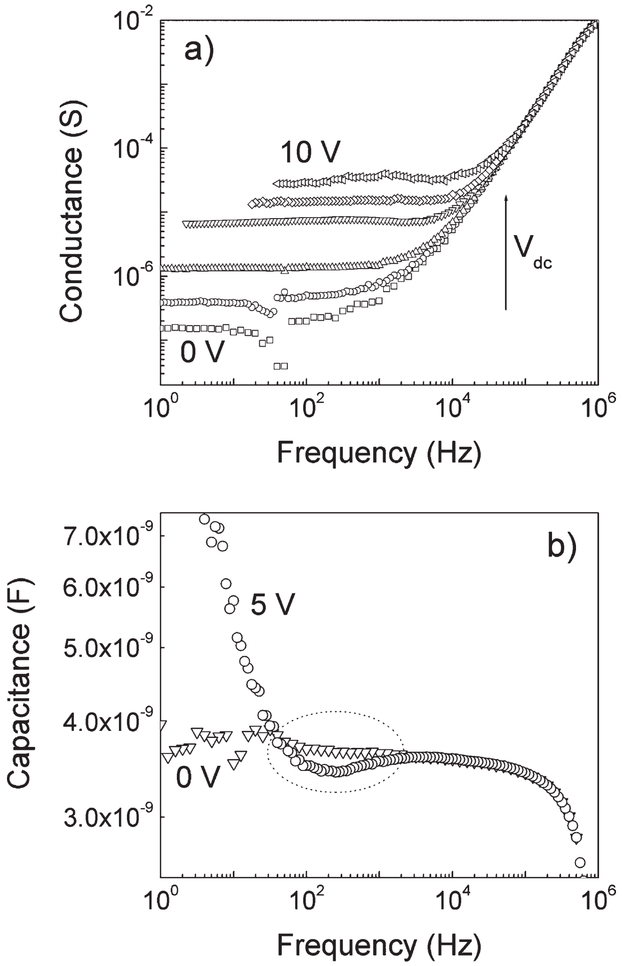

FIGURE 4 (a) Conductance spectra for an ITO/PEDOT:PSS/PPOPT/Al device, for dc bias (V_{dc}) values in the range of 0–10 V and with a step of 2 V. The arrow indicates the direction of increasing V_{dc}. (b) Capacitance spectra for an ITO/PEDOT:PSS/PPOPT/Al device at dc bias of 0 and 5 V.

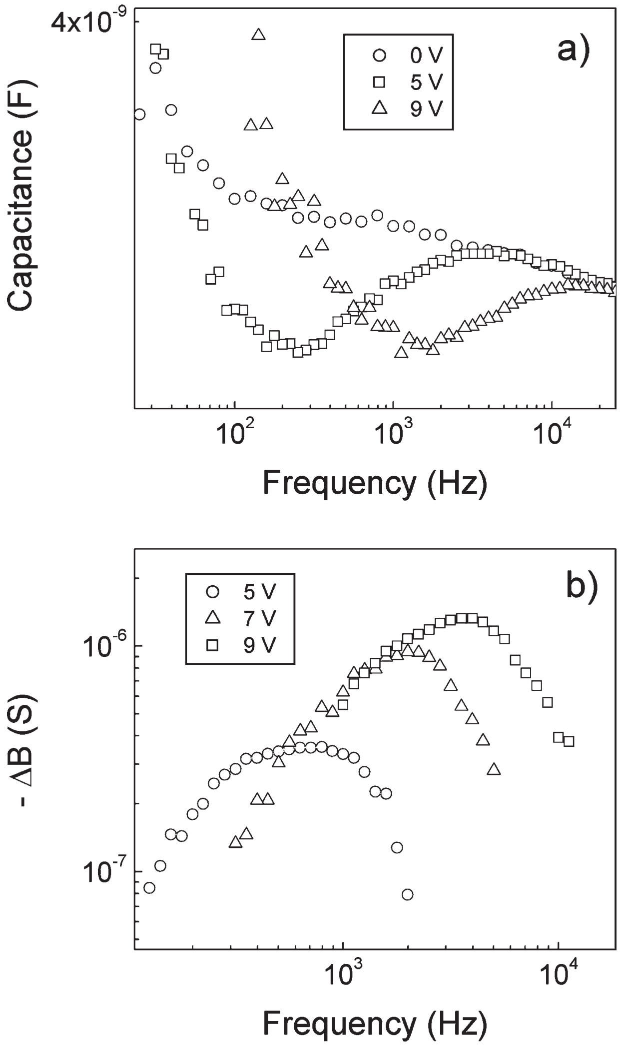

FIGURE 5 Intermediate-frequency range capacitance (a) and negative differential susceptance spectra (b) for an ITO/PEDOT:PSS/PPOPT/Al device at different dc bias (values shown in the figure).

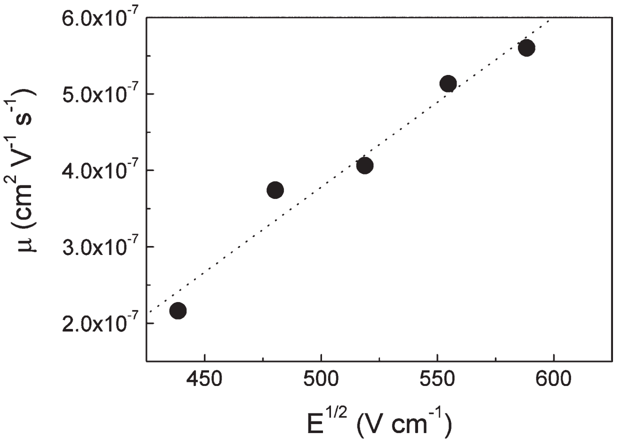

FIGURE 6 Square-root field-dependence of the average hole mobility for an ITO/PEDOT:PSS/PPOPT/Al device. The line represents the linear fit to the experimental data.

frequency range, with respect to zero-bias conditions, is often observed for disordered materials and has been attributed to trapping and subsequent detrapping of charge carriers.[20,21] The minima in the capacitance spectra are better displayed in Figure 5(a) and the figure also shows their shift toward higher frequency as the dc bias increases. The average transit times t_t of charge carriers can be easily evaluated from the negative differential subsceptance $-\Delta B$, obtained from capacitance through the following expression:

$$-\Delta B = -\omega(C - C_g) \tag{2}$$

where C_g, the geometrical capacitance of the sample, is given by the nearly frequency-independent capacitance value at $V_{dc} = 0$ [Fig. 4(b)]. It has been demonstrated that t_t is related to the frequency f_{max} at which $-\Delta B$ exhibits its maximum value through $f_{max} = kt_t^{-1}$, where for the empirical coefficient k, a value of 0.54 is usually assumed.[22] Peaks in $-\Delta B$ plots versus frequencies were clearly observed for PPOPT-based devices for V_{dc} of at least 5 V [Fig. 5(b)]. The peaks increase and shift toward higher frequencies as V_{dc} increases. The average hole mobility μ was calculated by using

$$\mu = \frac{d^2}{(V_{dc} - V_{bi})t_t} = \frac{d}{Et_t} \tag{3}$$

where d is the thickness of the polymer layer, V_{bi} is the built-in potential, based on the difference of the work functions of PEDOT:PSS and Al in the samples investigated in this study, and E is the applied electric field. The values of μ, calculated by assuming $V_{bi} = 1$ V, are displayed in Figure 6 as a function of the square root of E. Mobilities between 2.1×10^{-7} and 5.6×10^{-7} cm^2 V^{-1} s^{-1} were obtained at room temperature for thin film of PPOPT in the electric field range of 1.9×10^5–3.5×10^5 V cm^{-1}. These values are orders of magnitude lower than that recently reported for another phenyl-substituted polythiophene,[23] poly[3-(4-*n*-octyl)-phenylthiophene] (POPT).[12] Indeed, a bulk hole mobility of 1.0×10^{-4} cm^2 V^{-1} s^{-1} has been demonstrated for POPT films, comparable with that measured for regioregular poly(3-hexylthiophene) (P3HT) in the same experimental conditions. This indicates that the substitution of the solubilizing alkyl chain of P3HT with the phenyl–alkyl group of POPT leads to a similar organization of polymer chains in the solid state, profitable for charge transport. Differently, the 2′-pentyloxy-5′-(1‴-oxooctyl) phenyl substituent in PPOPT likely prevents interactions between adjacent polymer chains due to its steric effect, resulting in a strong negative effect for charge transport.

The rough linear trend of the plot displayed in Figure 6 indicates that hole mobility in PPOPT thin films follows the Poole-Frenkel expression[24]

$$\mu = \mu_0 \exp(\gamma\sqrt{E}) \tag{4}$$

where μ_0 denotes the mobility at zero field and γ is the parameter describing how strong is the field dependence. The parameters for the Poole–Frenkel fit to mobility data of Figure 6 are $\mu_0 = 1.77 \times 10^{-8}$ cm^2 V^{-1} s^{-1} and $\gamma = 6.0 \times 10^{-3}$ (V cm^{-1})$^{-1/2}$. The value of γ is rather high, indicating a strong dependence of hole mobility on electric field.

CONCLUSIONS

A novel phenyl-substituted polythiophene has been synthesized and its electrochemical and optical properties have been investigated. PPOPT shows an optical energy gap of 2.0 eV and its relatively high quantum yield of PL in the solid state (0.11), equal to that measured in diluted solution, indicates small interactions between polymer chains. This is attributed to the long alkyl chain of the 2′-pentyloxy-5′-(1‴-oxooctyl) phenyl substituent which causes twisting of the phenyl ring out of the plane and leads to poor electronic interaction of the thiophene chains.

This picture is confirmed by the investigation of the bulk transport properties of PPOPT. Hole mobility in thin films of PPOPT was found to be moderate (of the order of 10^{-7} cm^2 V^{-1} s^{-1} for an electric field of 10^5 V cm^{-1}) and strongly field activated, as indicated by the rather high value [6.0×10^{-3} (V cm^{-1})$^{-1/2}$] of the Poole–Frenkel parameter describing the field dependence of mobility. This study demonstrates the importance of substituents for the π conjugation of the aromatic system of polymer materials and how dramatically they can affect the electronic properties.

S.E. Debebe acknowledges the "Programme for Training and Research in Italian Laboratories (TRIL)," The Abdus Salam International Centre for Theoretical Physics (ICTP), for financial support (budget code 421.FITU.21.G). This work was partially supported by ENI S.p.A. and by the CNR PM.P04.010 MACOL.

REFERENCES AND NOTES

1 Handbook of Conducting Polymers; Skotheim, T. A.; Elsenbaumer, R. L.; Reynolds, J. R., Eds.; Marcel Dekker: New York, 1998.

2 Po, R.; Maggini, M.; Camaioni, N. J Phys Chem C 2010, 114, 695–706.

3 Yamashita, Y. Sci Technol Adv Mater 2009, 10, 024313.

4 Andersson, M. R.; Berggren, M.; Inganas, O.; Gustafsson G.; Gustafsson-Carlberg, J. C.; Selse, D.; Hjertberg, T.; Wennerstroem O. Macromolecules 1995, 28, 7525–7529.

5 Handbook of Thiophene-Based Materials: Applications in Organic Electronics and Photonics; Perepichka, I. F.; Perepichka, D. F., Eds.; Wiley: New York, 2009; Vol. 1.

6 Joansson, T.; Mammo, W.; Svensson, M.; Andersson, M. R.; Inganas, O. J Mater Chem 2003, 13, 1316–1323.

7 Perepichka, I. F.; Perepichka, D. F.; Meng, H.; Wudl, F. Adv Mater 2005, 17, 2281–2305.

8 Zhang, F. L.; Svensson, M.; Andersson, M. R.; Maggini, M.; Bucella, S.; Menna, E.; Inganas, O. Adv Mater 2001, 13, 1871–1874.

9 (a) deMello, J. C.; Wittman, H. F.; Friend, R. H. Adv Mater 1997, 9, 230–232; (b) Barbieri, A.; Accorsi, G. European Photochemistry Association (EPA) Newsletter, December 2006, 26–34.

10 Gritzner, G. K. J. Pure Appl Chem 1984, 56, 461–466.

11 Andersson, M. R.; Selse, D.; Berggren, M.; Järvinen, H.; Hjertberg, T.; Inganäs, O.; Wennerstörm, O.; Österholm, J. E. Macromolecules 1994, 27, 6503–6506.

12 Pei, Q.; Järvinen, H.; Österholm, J. E.; Inganäs, O.; Laakso, J. Macromolecules 1992, 25, 4297–4301.

13 Jiang, X.; Osterbacka, R.; Korovyanko, O.; An, C. P.; Horowitz, B.; Janssen, R. A. J.; Vardeny, Z. V. Adv Funct Mater 2002, 12, 587–597.

14 McCullough, R. D.; Lowe, R. D.; Jayraman, M.; Anderson, D. L. J Org Chem 1993, 58, 904–912.

15 Aasmundtveit, K. E.; Samuelsen, E. J.; Mammo, W.; Svensson, M.; Andersson, M. R.; Pettersson, L. A. A.; Inganas, O. Macromolecules 2000, 33, 5481–5489.

16 Kanemoto, K.; Sudo, T.; Akai, I.; Hashimoto, H.; Karasawa, T.; Aso, Y.; Otsubo, T. Phys Rev B 2006, 73, 235203.

17 Theander, M.; Inganas, O.; Mammo, W.; Olinga, T.; Svensson, M.; Andersson, M. R. J Phys Chem B 1999, 103, 7771–7780.

18 Trasatti, S. Pure Appl Chem 1986, 58, 955–966.

19 Campbell, I. H.; Hagler, T. H.; Smith, D. L.; Ferraris, J. P. Phys Rev Lett 1996, 76, 1900–1903.

20 Kassing, R. Phys Stat Sol (a) 1975, 28, 107–117.

21 Poplavskyy, D.; So, F. J Appl Phys 2006, 99, 033707.

22 Blom, P. W. M.; Martens, H. C. F.; Huiberts, J. N. Synth Met 2001, 121, 1621–1624.

23 Woo, C. H.; Holcombe, T. W.; Unruh, D. A.; Sellinger, A.; Frechert, J. M. Chem Mater 2010, 22, 1673–1679.

24 (a) Poole, H. H. Philos Mag 1916, 33, 112–129; (b) Frenkel, J Phys Rev 1938, 54, 647–648.